

Preparation and characterization of carbonyl iron/poly(butylcyanoacrylate) core/shell nanoparticles

J.L. Arias^a, V. Gallardo^a, F. Linares-Molinero^a, A.V. Delgado^{b,*}

^a *Department of Pharmacy and Pharmaceutical Technology, Faculty of Pharmacy, University of Granada, Spain*

^b *Department of Applied Physics, Faculty of Sciences, University of Granada, Spain*

Received 6 September 2005; accepted 3 March 2006

Available online 9 March 2006

Abstract

In this article a method is described to prepare composite colloidal nanoparticles, consisting of a magnetic core (carbonyl iron) and a biodegradable polymeric shell [poly(butylcyanoacrylate) or PBCA]. The method is based on the so-called anionic polymerization procedure, often used in the synthesis of poly(alkylcyanoacrylate) nanospheres designed for drug delivery. Interest of this investigation is based upon the fact that the heterogeneous structure of the particles can confer them both the possibility to respond to external magnetic fields and to be used as drug carriers. In order to investigate to what extent do the particles participate of this mixed properties, we compare in this work the physical characteristics (structure, chemical composition, specific surface area and surface electrical and thermodynamic properties) of the core/shell particles with those of both the nucleus and the coating material. This preliminary study shows that the mixed particles display an intermediate behavior between that of carbonyl iron and PBCA spheres. Electrophoretic mobility measurements as a function of pH and as a function of KNO₃ concentration, show a great similarity between the core/shell and pure polymer nanoparticles. Similarly, a surface thermodynamic study performed on the three types of particles demonstrated that the electron-donor component of the surface free energy of the solids is very sensitive to the surface composition. In fact, a measurable decrease of such component is found for core/shell particles as compared to carbonyl iron. We also analyzed the influence of the relative amounts of polymer and carbonyl iron on the characteristics of the composite particles: data on the coating thickness, the amount of polymer bound to the magnetic nuclei, the redispersibility characteristics of the suspensions and the surface electrical and thermodynamic properties, suggest that the optimal synthesis conditions are obtained for a 4/3 initial monomer/carbonyl iron weight ratio.

© 2006 Elsevier Inc. All rights reserved.

Keywords: Biodegradable polymers; Carbonyl iron; Coating; Core/shell colloidal particles; Drug delivery systems; Electrophoresis; Magnetic carrier technology; Magnetic colloids; Magnetic targeted carriers; Poly(butylcyanoacrylate); Surface thermodynamics

1. Introduction

Because of their unique physical properties (regarding size and shape, magnetic characteristics, biocompatibility, etc.), magnetic colloids in the submicrometric and nanometric size ranges have found increasing and very promising applications in the biomedical field. Some of them include: cell therapy (cell separation and labelling), tumor treatment by hyperthermia, magnetic resonance imaging (MRI) contrast enhancement, tissue repair, and, particularly, drug delivery [1–3].

Drug delivery systems are designed to ensure the distribution of drugs in the organism in a manner such that its major fraction interacts exclusively with the target tissue at the cellular or subcellular level. Magnetically-controlled drug targeting is currently one of the most active areas of cancer research and one of the principal possibilities of active drug targeting, that will allow the guidance of drug carriers to specific cells in a manner that differs from its normal distribution in the organism, selectively delivering anticancer drug molecules to the diseased site without a concurrent increase in its level in healthy tissues. Those magnetic systems can improve the outcome of chemotherapy by allowing: (i) the maximum fraction of the delivered active agent to react exclusively with the cancer cells without adverse effects to the normal cells; and (ii) preferential

* Corresponding author. Fax: +34 958 243214.
E-mail address: adelgado@ugr.es (A.V. Delgado).

distribution of drug to the cancer cells, limiting systemic drug concentrations and, importantly, avoiding normal tissue clearance with the aid of an external magnetic field [4–6].

After injecting a magnetically susceptible material, drug targeting is obtained with a magnet of sufficient strength and focus to retain the particles in a flow field, such as that found in the vasculature feeding tumor. An optimum particle would extravasate into the tissue and be physically retained [6–8].

Despite the promise of magnetic targeting, shown by lots of animal studies, definitive problems can be identified in the application to humans: (i) poor targeting at a deep site within the body (>2 cm); (ii) poor retention of the magnetic carriers when the magnet is removed; and (iii) poor drug binding and release characteristics of the carriers. However, the number of promising human clinical trials is rising in the recent years [4,7,9].

The magnetically susceptible carrier that we describe in this article is composed of a magnetic nucleus (carbonyl iron) and a biodegradable polymeric shell [poly(butylcyanoacrylate), PBCA], in order to take advantage of the properties of its two components. The magnetic core could allow to direct particles to the specified location and maintain them there by means of magnetic external fields. The polymeric shell could transport the drug and release it during its biodegradation. In previous works [10,11], we have described procedures to obtain and characterize a similar family of particles formed by a magnetite spherical nucleus covered by a shell of poly(ethyl-2-cyanoacrylate), and its application to 5-fluorouracil drug loading.

Carbonyl iron (Fe^0) is a well-known material, a unique form of elemental iron (because of its small particle size), properly characterized in many aspects, that was chosen to serve as the magnetic nuclei and to set the size of the particles. Carbonyl iron is made by treating iron with carbon monoxide (CO) under heat and pressure. The resulting pentacarbonyl iron [$\text{Fe}(\text{CO})_5$] is then decomposed under controlled conditions, and yields CO and iron powder that is extremely pure and produced in the form of almost perfect spheres with an average particle size of 5–6 μm [12]. Its toxicity has been demonstrated to be quite low (LD_{50} : 50 g/kg, see Ref. [12]), and corroborated by several studies [13–15]. Concerning the biodegradability of the carbonyl iron used in this work, and because of its average diameter of 470 ± 180 nm (see below), most particles will remain in the body, being finally eliminated mainly by renal filtration [16].

Poly(butylcyanoacrylate) or PBCA was chosen as the polymer to build the biodegradable shell on the magnetic particles. Because of their properties (including mechanical, biodegradability, biocompatibility, drug compatibility, see Refs. [17,18]), polyalkylcyanoacrylates have produced very promising results as polymeric substrates in the preparation of injectable nanoparticle delivery systems. Interestingly, one of its most promising therapeutic applications is in antineoplastic therapy, because of their ability to reverse *in vitro* tumor-cell resistance to anticancer drugs [19–21]. These particles compare favorably to other biodegradable polymers such as alginate, poly(lactide) or poly(lactide-co-glycolide) [22]. Their toxicity, although low LD_{50} of polyisobutylcyanoacrylate (PIBCA)

in rats: 242 mg/kg; LD_{50} of polyhexylcyanoacrylate (PHCA) in rats: 585 mg/kg, see Refs. [23,24], even after histological examinations [25], can be important because they have a fast degradation rate as compared to other polymers used in drug delivery, and yield rather toxic biodegradation products [alcohol and poly(cyanoacrylic acid)]. However, in the case of long-term treatments, the use of rapidly degrading cyanoacrylate carriers appears more appropriate in order to avoid overloading the cells with slowly degrading polyesters [26].

Considering that, as demonstrated in Ref. [23], the inclusion of iron oxides (i.e., magnetite, Fe_3O_4) in poly(alkylcyanoacrylate) substrate does not affect the toxicity of the latter (LD_{50} of Fe_3O_4 /PIBCA in rats: 245 mg/kg), it seemed of interest to investigate on the applicability of carbonyl iron/polymer composites in the pharmaceutical technology. In this work we describe a technique for the preparation of spherical mixed particles, consisting of a carbonyl iron nucleus and a PBCA shell. The characteristics of the coating will be analyzed by comparing the infrared absorption spectra, and the electrical, thermodynamic and chemical surface properties of the composite particles, to those of the pure carbonyl iron and polymer colloids.

2. Materials and methods

2.1. Materials

All chemicals used were of analytical quality from Panreac, Spain, except for carbonyl iron (BASF, Germany), butylcyanoacrylate (a gift from Henkel Loctite Technology Centre Europe, Ireland), formamide (Aldrich, USA), diiodomethane (Fluka, Germany) and, KOH and acetone (Merck, Germany). Water used in the experiments was of Milli-Q quality (Milli-Q Academic, Millipore, France).

2.2. Methods

2.2.1. Preparation of carbonyl iron, poly(butylcyanoacrylate) and carbonyl iron/PBCA (core/shell) nanoparticles

Different selection methods for the nanoparticles of carbonyl iron provided were studied, in order to reduce the size heterogeneity and the number of the particles with a diameter over 1 μm in the original sample. Carbonyl iron suspensions [0.3% (w/v)] were subjected to filtration in a stirred filtration cell with a membrane of 1 μm , centrifugation at a minimum centrifugation rate (100 rpm) and magnetic separation with a permanent magnet, obtaining negligible outputs of magnetic nanoparticles with the desired properties. The only method with a reasonable output (see below) was gravitational separation. Briefly, this method involves the sonication of 0.3% (w/v) carbonyl iron suspensions in water during 5 min before leaving those suspensions to settle under gravity. The conductivity of the supernatant was ≈ 1 $\mu\text{S}/\text{cm}$, and no other solids but carbonyl iron were in the suspension. The particles were then dried at 60 °C in a vacuum oven and stored until their use. The optimization of the method involves the study of the influence of the sedimentation time and the amount of supernatant taken from the suspension. Therefore, the experiments were carried out for sedimentation

times between 0 and 90 min, with the extraction of 100 mL of supernatant; and for supernatant volumes between 100 and 300 mL, after 60 min sedimentation. The experiments were repeated at least three times on independent samples in all cases.

The method followed for the synthesis of colloidal nanospheres of PBCA is the emulsion/polymerization method, in which the mechanism of polymerization is an anionic process initiated by covalent bases present in the medium [17]. In detail [10,11], the monomer (up to 1% w/v) was added dropwise to 50 mL of a 10^{-4} N HCl aqueous solution containing a 1% (w/v) of the surfactant Dextran-70. Stirring at 1000 rpm was maintained during the 2 h of the polymerization reaction, which was terminated by adding 1 mL of a 0.1 N KOH solution. A whitish suspension was obtained which was then subjected to a cleaning procedure that included repeated cycles of centrifugation (20,000 rpm, Centrikon T-124 high-speed centrifuge, Kontron, France) and redispersion in Milli-Q water. In order to ensure that the suspension was sufficiently clean, the conductivity of the supernatant was measured. The polymer particles were dried at 35 °C in a vacuum oven and stored in dry polyethylene containers until their use.

Finally, the procedure followed to obtain the composite nanoparticles was very similar to the one described for the polymer spheres, except that the polymerization medium was a 0.75% w/v carbonyl iron suspension in 10^{-4} N HCl solution [11]. Cleaning was achieved by repeated magnetic separation and redispersion in Milli-Q water. After approximately 3 cycles, the conductivity of supernatants indicated that the suspensions were clean of both unreacted chemicals and non-magnetic polymer particles. In order to analyze the influence of the relative amounts of polymer and carbonyl iron on the characteristics of the material, the synthesis was repeated with monomer/carbonyl iron proportions ranging from 4/3 to 4/1. Lower monomer proportions were not used because results from a previous study using those weight ratios of a poly(alkylcyanoacrylate) monomer produced too many uncovered magnetic particles and a very thin polymer shell, mainly located in the contact regions between the particles [10].

2.2.2. Characterization methods

The size and shape of the different particles synthesized were deduced from TEM pictures using a Zeiss EM 902 (Germany) transmission electron microscope set at 80 kV accelerating voltage. Prior to observation, a dilute (approx. 0.1% w/v) suspension of the particles was sonicated for 5 min, and drops of the suspension were placed on copper grids with formvar film. The grids were then dried at 40 °C in a convection oven.

Fourier transform infrared spectrometry (FTIR) (Nicolet 20 SXB infrared spectrometer, USA) data with a resolution of 2 cm^{-1} were used for the characterization of the chemistry of the three types of particles (carbonyl iron, polymer and core/shell nanoparticles).

^1H and ^{13}C nuclear magnetic resonance analyses (Bruker AM-300, USA) were used to investigate the molecular structure of the polymer PBCA, using deuterated chloroform (CDCl_3) as solvent.

Specific surface areas of the solids were obtained by multipoint BET nitrogen adsorption in a Quantasorb Jr. of Quantachrome (USA). The carrier gas in this device is helium, and adsorption experiments were performed with 10, 20 and 30% nitrogen/helium mixtures. The sample mass used was 0.5 g (polymer particles), 0.4 g (carbonyl iron), and 0.6 g (composite particles). The experiments were repeated at least three times on independent samples in all cases.

The magnetic properties of the carbonyl iron and composite particles (first magnetization curve and hysteresis cycle) were determined with a Manics DSM-8 vibrating magnetometer, at room temperature.

The surface electrical properties of the different particles were analyzed by electrophoresis measurements as a function of both pH and KNO_3 concentration using a Malvern Zetasizer 2000 (England) electrophoresis device. Measurements were performed at 25.0 ± 0.5 °C. These data were very useful in ascertaining the efficiency of the coating for different initial Fe/polymer mass ratios. Finally, the differences between the surface properties of the three kinds of particles (nuclei, polymer, and composite) were also investigated by performing a surface thermodynamic analysis. Our starting point is the model developed by van Oss and his group [27–29], according to which the total surface free energy of any material i is the sum of two contributions [27,28]:

$$\gamma_i^{\text{TOT}} = \gamma_i^{\text{LW}} + \gamma_i^{\text{AB}} = \gamma_i^{\text{LW}} + 2\sqrt{\gamma_i^+ \gamma_i^-} \quad (1)$$

one of which, γ_i^{LW} , is the non-polar Lifshitz–van der Waals component, and the second one, γ_i^{AB} or acid–base component, is related to the electron-donor (γ_i^-) and electron-acceptor (γ_i^+) characteristics of the material. Similarly, the interfacial solid/liquid free energy, $\gamma_{\text{SL}}^{\text{TOT}}$, and its LW and AB components ($\gamma_{\text{SL}}^{\text{LW}}$, $\gamma_{\text{SL}}^{\text{AB}}$, respectively) are related to the surface free energies of both the solid (subscripts S) and the liquid (subscripts L):

$$\begin{aligned} \gamma_{\text{SL}}^{\text{TOT}} = \gamma_{\text{SL}}^{\text{LW}} + \gamma_{\text{SL}}^{\text{AB}} = \gamma_{\text{SL}}^{\text{LW}} + 2\sqrt{\gamma_{\text{S}}^+ \gamma_{\text{L}}^-} \\ + 2\sqrt{\gamma_{\text{S}}^- \gamma_{\text{L}}^+} - 2\sqrt{\gamma_{\text{S}}^+ \gamma_{\text{L}}^-} - 2\sqrt{\gamma_{\text{S}}^- \gamma_{\text{L}}^+}. \end{aligned} \quad (2)$$

Using the Young equation [30], these quantities can be related to the contact angle θ between the liquid and the solid:

$$(1 + \cos \theta) \gamma_{\text{L}}^{\text{TOT}} = 2\sqrt{\gamma_{\text{S}}^{\text{LW}} \gamma_{\text{L}}^{\text{LW}}} + 2\sqrt{\gamma_{\text{S}}^+ \gamma_{\text{L}}^-} + 2\sqrt{\gamma_{\text{S}}^- \gamma_{\text{L}}^+}. \quad (3)$$

The three unknowns ($\gamma_{\text{S}}^{\text{LW}}$, γ_{S}^+ , and γ_{S}^-) can be obtained by solving the resulting system of three equations if one measures the contact angles of three liquids of known $\gamma_{\text{L}}^{\text{LW}}$, γ_{L}^+ , and γ_{L}^- . In our case, we used water ($\gamma_{\text{L}}^{\text{LW}} = 21.8$, $\gamma_{\text{L}}^+ = \gamma_{\text{L}}^- = 25.5\text{ mJ/m}^2$), formamide ($\gamma_{\text{L}}^{\text{LW}} = 39.0$, $\gamma_{\text{L}}^+ = 2.28$, $\gamma_{\text{L}}^- = 39.6\text{ mJ/m}^2$) and diiodomethane ($\gamma_{\text{L}}^{\text{LW}} = 50.8$, $\gamma_{\text{L}}^+ = \gamma_{\text{L}}^- = 0\text{ mJ/m}^2$; all data taken from Ref. [27]). Measurements were performed with a Ramé–Hart 100-00 goniometer (USA). We measured the contact angles of the three liquids on pellets (radius: 1.3 cm) obtained by compressing the dry powders in a Spexac hydraulic press set to 10 Ton during 5 min.

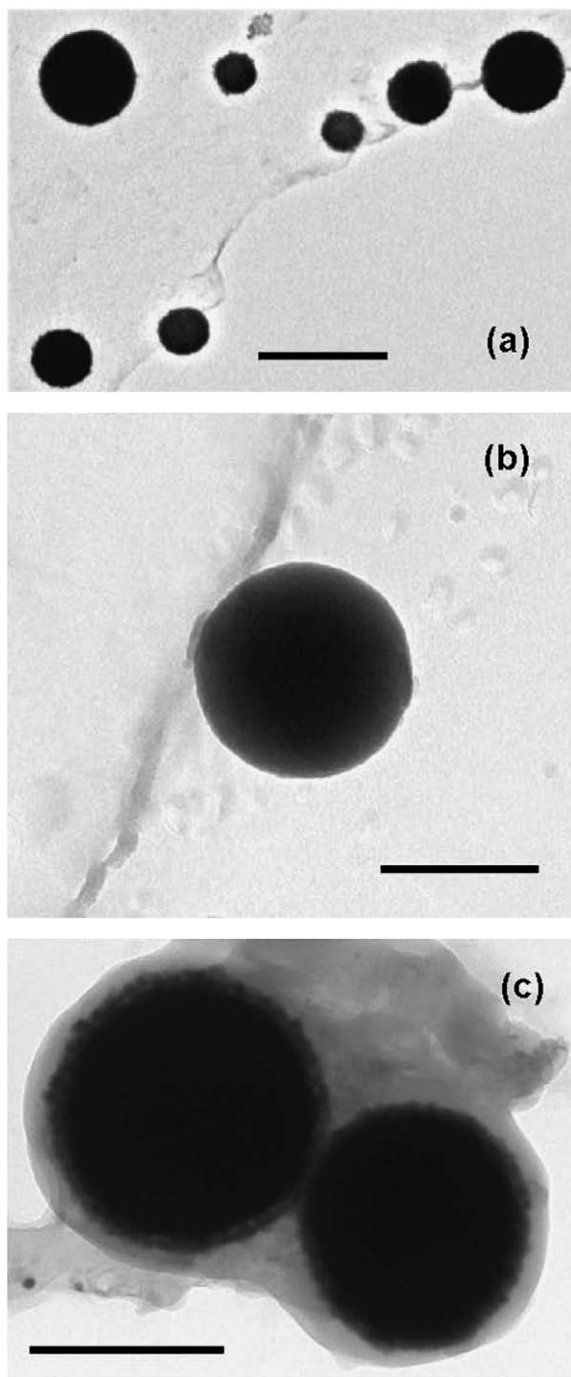


Fig. 1. Transmission electron microscopy photographs of carbonyl iron (a), poly(butylcyanoacrylate) (b), and composite particles (c). Bar lengths: 1 μm (a), 500 nm (b), and 400 nm (c).

3. Results and discussion

3.1. Particle geometry

Fig. 1a shows TEM pictures of the carbonyl iron particles obtained using the optimized method to achieve the minimum size heterogeneity and the maximum number of magnetic particles with diameter under 1 μm (60 min sedimentation, and the upper 10 mm of supernatant taken; 1 L flasks with an internal diameter of about 90 mm were used for these sepa-

Table 1

Relative amount of polymer bound to carbonyl iron (mass of polymer per unit mass of carbonyl iron), coating thickness and redispersibility characteristics of the composite particles obtained for different relative initial amounts of monomer and carbonyl iron

Initial monomer/magnetite weight ratio	Relative weight of coating polymer	Coating thickness (nm)	Redispersibility
4/3	0.714 ± 0.002	25 ± 12	Good
4/2	1.437 ± 0.004	47 ± 24	Fair
4/1	0.193 ± 0.006	35 ± 10	Difficult

rations); as observed, they are spherical and with a not very broad size distribution (average diameter and standard deviation: 470 ± 180 nm). Fig. 1b corresponds to the pure polymer particles, showing a spherical shape and 550 ± 120 nm in diameter.

A qualitative analysis of the effect of changing the relative amounts of carbonyl iron and monomer in the dispersion medium on the structure of the particles was achieved by means of TEM pictures. Fig. 1c shows the particles synthesized when the initial monomer/carbonyl weight ratio was 4/3. Their average diameter and standard deviation (520 ± 210 nm) indicate again a moderately polydisperse system, and the picture clearly shows that the carbonyl iron particles are covered by a polymer shell ≈ 25 nm thick. No experiments were carried out using lower monomer proportions (1/4 to 4/4), because a very thin polymer shell and an increment of the uncovered carbonyl iron particles is expected, as studied for magnetite particles [10]. On the contrary, when the amount of monomer is in excess of that of carbonyl iron (4/3 to 4/1) all the particles appear covered. In Table 1 we show the thickness of the coating, the amount of polymer bound to carbonyl iron, and the redispersibility characteristics of the suspensions. The first quantity was determined from TEM pictures as described; the polymer actually bound to the particles was obtained from the weight difference between the coated carbonyl iron particles and the bare ones. Finally, the assessment of redispersibility was performed qualitatively, by simple visual inspection of the turbidity after sonication of a sedimented suspension. As observed, the amount of PBCA incorporated to the particles increases consistently when the monomer/carbonyl iron ratio is raised. Concerning the thickness of the polymer coating, note how an excess of initially added monomer does not necessarily lead to a more efficient coating of carbonyl iron. The poor redispersion achieved when the monomer/carbonyl iron ratio is above 4/3 is an indication of the formation of polymer films that are virtually impossible to destroy by non-chemical methods.

Considering the final potential use of these particles, it is interesting to comment on the significance of the sizes obtained for the core/shell particles. First of all, the magnetic responsiveness of the particles will be stronger the larger their size (and hence their magnetic moment). Nevertheless, the size affects not only to the magnetic (or other physical) properties, but, most important, to the fate of the particles once they are injected in the body. According to Gupta and Gupta [3], particles with diameters in excess of 200 nm will easily be sequestered by the spleen and removed by the cells of the reticuloendothelial

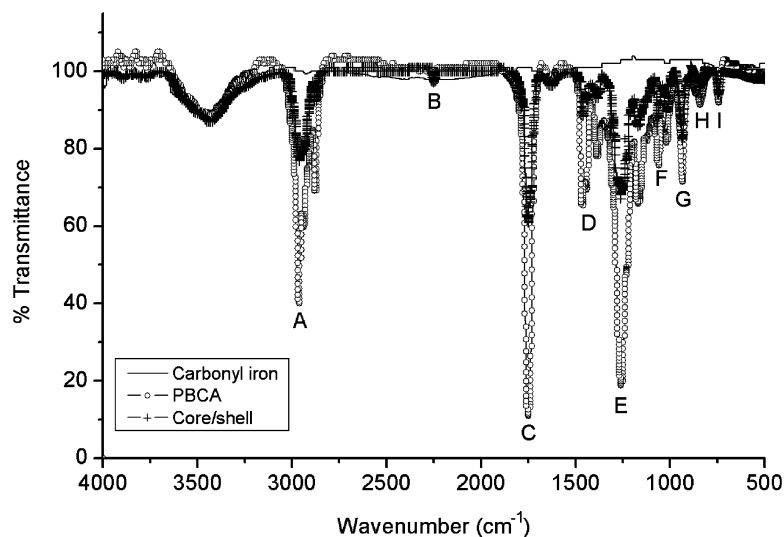


Fig. 2. Infrared spectra of carbonyl iron, poly(butylcyanoacrylate), and mixed particles. The main groups identified are: (A) C–H stretching; (B) $C\equiv N$ stretching; (C) Normal dimeric carboxylic C=O stretching; (D) C–H bending; (E) and (F) C–CO–C stretching and bending; (G) O–C–C bending of esters of primary alcohols; (H) Medium band characteristic of alkanes; (I) CH_2 rocking vibration characteristic of $-CH_2-$ long chains. The band around 3000 cm^{-1} corresponds to the moisture content of the samples.

system. On the opposite side, very small (under 10 nm) carriers will be rapidly cleared after their extensive extravasation. Hence, the ideal size range for colloidal carriers to be spread systemically is around 10–100 nm. However, it must be taken into account that the therapeutic action can take place already if the particles are retained by the applied magnetic field in the capillaries feeding the tumor, and release the drug, which, in turn, will diffuse from the capillary wall into the tissue. With such mechanisms in mind, it is not the size of the particles only but, equally important, the molecular weight of the therapeutic drug that is essential in the overall process [31]. If the action of the drug carriers require extravasation, some authors suggest that sizes below $1\text{ }\mu\text{m}$ may already be suitable for that process [3,31]. Thus, Goodwin et al. [32] found (after magnetic field switch off) extravasation of particles with size distributions in the range 0.5–5 μm .

The surface area of carbonyl iron is $1.37 \pm 0.16\text{ m}^2/\text{g}$, which is higher than the one for the polymer ($0.47 \pm 0.19\text{ m}^2/\text{g}$) and the composite particles ($0.62 \pm 0.13\text{ m}^2/\text{g}$). The similarity between the surface areas of the polymer and core/shell particles points to an efficient coating, given that the particles (iron, polymer, composite) have similar sizes. Thus, the changes observed in the surface area of the nuclei after covering them with polymer must reflect a true change in the physical properties of the surface of the iron nucleus upon sufficient coverage by the polymer.

3.2. Chemical composition of the particles

Fig. 2 shows the infrared spectra of the three types of particles. The most significant bands have been identified by comparison with data in Refs. [10,33]. It can be observed that all the bands of the polymer are present in the spectrum of the composite particles, a clear indication that the shell observed in Fig. 1c is indeed PBCA coating.

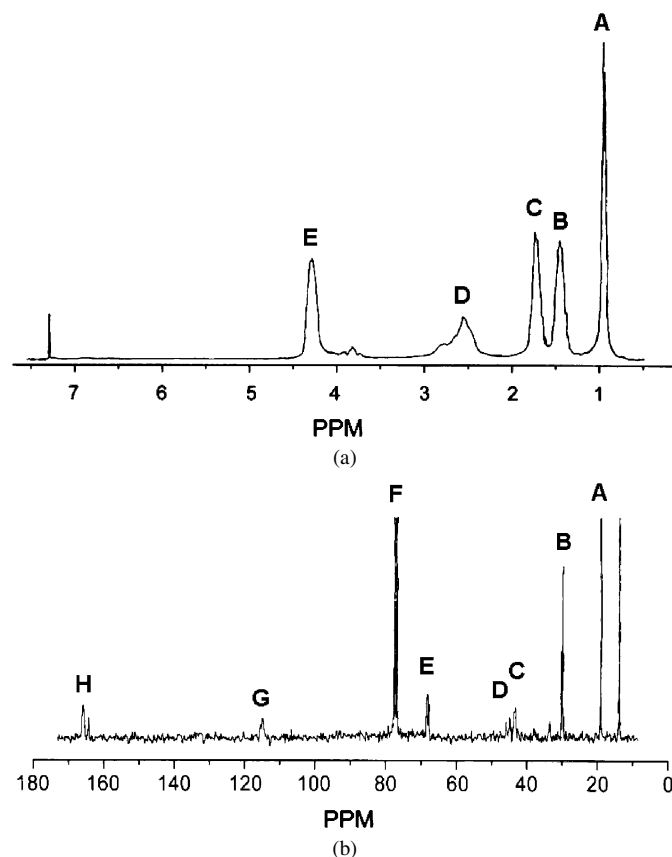


Fig. 3. ^1H -NMR spectra (a) and ^{13}C -NMR spectra (b) of poly(butylcyanoacrylate).

Proton NMR data (Fig. 3a) display five well-defined peaks for analysis: Bands A (0.97 ppm), C (1.74 ppm) and E (4.27 ppm) correspond to the protons localized in α -, β -, and γ -position with respect to the ester group, respectively. Finally, peaks B and D (1.46 and 2.56 ppm) are generated by

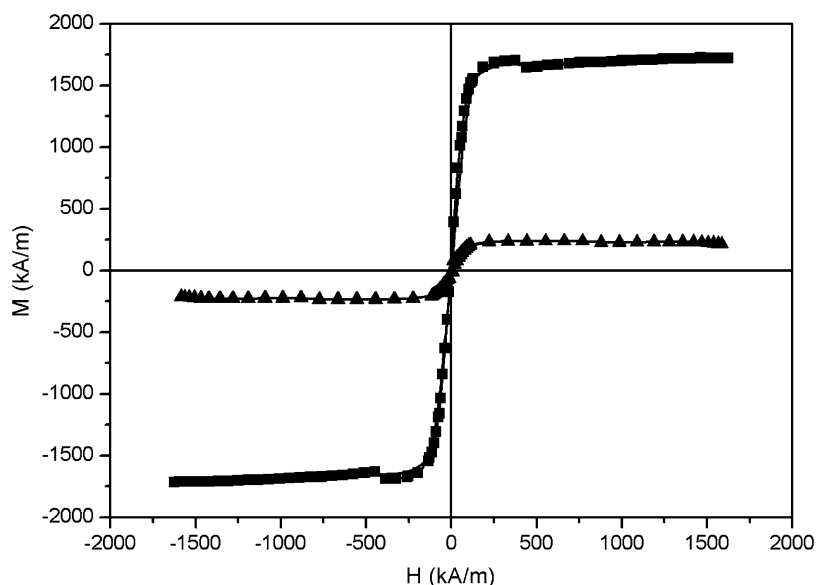


Fig. 4. Hysteresis cycles of the carbonyl iron (■) and core/shell nanoparticles (▲).

the hydrogen of the methylene groups constituting the backbone polymeric chain. Results in Refs. [11,34], corresponding to polymers of the same family, poly(ethyl-2-cyanoacrylate) and poly(isobutylcyanoacrylate), show a great similarity to ours.

The ^{13}C NMR spectrum (Fig. 3b) shows a number of bands that have also been found for poly(isobutylcyanoacrylate): Band A (18.96 ppm) is characteristic of the methyl group of the side chain. Bands B (29.81 ppm) and E (68.32 ppm) correspond to the protons localized in β - and γ -position with respect to the ester group, respectively. Band C (43.24 ppm) belongs to the tetrasubstituted carbon of the backbone, of which the methylenic carbon gives rise to band D (44.80 ppm). Band F (77.09 ppm) corresponds to the solvent. Finally, bands G (114.72 ppm) and H (165.68 ppm) are characteristic of the cyano and ester groups, respectively.

3.3. Magnetic properties

Fig. 4 shows the hysteresis cycles of both the carbonyl iron nuclei and the composite particles. Both iron and mixed particles show a soft magnetic behavior, and in fact the increasing and decreasing branches of the hysteresis cycles are hardly distinguishable, considering the sensitivity of our magnetometer. As previously observed in the case of magnetite/poly(ethyl-2-cyanoacrylate) core/shell nanoparticles [11], the magnetic behavior of composite nanoparticles is similar to that of the nuclei, except that the polymeric shell reduces the magnetization of the sample. From the linear portions (low field) of the curves in Fig. 4, we could estimate the initial susceptibility, $\chi_i = 20.46 \pm 0.19$ for carbonyl iron and $\chi_i = 2.33 \pm 0.11$ for the composite nanoparticles. It is also significant the reduction of saturation magnetization brought about by the polymer layer: 1582 ± 5 kA/m for carbonyl iron (close to published data obtained with $6 \mu\text{m}$ particles, see Ref. [35]), and 223.7 ± 1.1 kA/m for core/shell particles. In spite of this expected reduction in

magnetic strength, the composite particles meet the proposed requirements: their surface is comparable to that of the pure polymer, but they have the property of being magnetizable, so they constitute an ideal candidate to be used for magnetic drug delivery.

3.4. Electrokinetic characterization

We first focussed our study on the effect of pH on the electrophoretic mobility, u_e , and zeta potential, ζ , of the particles. Thus, Fig. 5 shows both quantities as a function of pH in the presence of 10^{-3} M KNO_3 , for particles obtained with all the monomer/carbonyl iron ratios investigated, together with pure polymer and iron particles. The theory of O'Brien and White [36] was used to convert u_e into ζ values. Note that carbonyl iron particles show a well defined isoelectric point (pH_{iep} or pH of zero potential) close to $\text{pH} = 4.5$. It is worth considering the origin of the surface charge of the metal particles and its dependence with pH. In an extensive study of the isoelectric points of several metals, Kallay et al. [37] demonstrated the similarities existing between the isoelectric points of metals and of their corresponding oxides. Such similarities are based upon the fact that the surface charge of the metal/solution interface is originated by the amphoteric thin oxide layer whose formation cannot be avoided in oxidizing environments. In particular, the isoelectric point of iron is similar to that of hematite ($\alpha\text{-Fe}_2\text{O}_3$). Since this oxide is known to have its zero zeta potential at a pH_{iep} close to 7–8 [38], it can be expected that the iron particles will display a positive surface charge at the pH of the synthesis of the core/shell particles ($\text{pH} \approx 4$).

Such a behavior is not found in PBCA particles, that have a negative surface charge for almost the whole pH range studied. It is only at $\text{pH} < 3$ that the zeta potential of this metal can attain zero values. This is due to the low degree of dissociation of free acrylic groups at this pH [39]. Because of

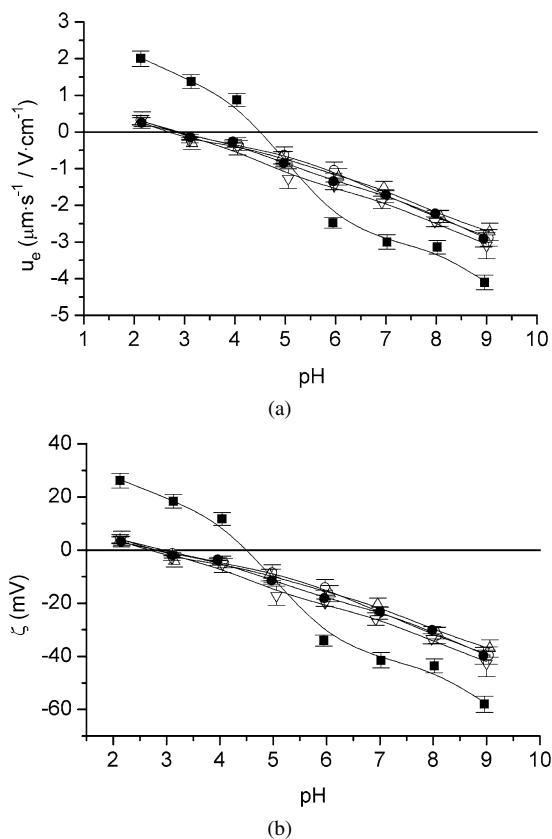


Fig. 5. Electrophoretic mobility (a) and zeta potential (b) of carbonyl iron (■), poly(butylcyanoacrylate) (●) and composite particles [of different initial monomer/carbonyl iron weight ratio: 4/3 (▽), 4/2 (△) and 4/1 (○)] as a function of pH in the presence of 10^{-3} M KNO_3 .

such large differences between the electrophoresis of nuclei and polymer, this electrokinetic technique is a very useful tool for qualitatively checking the efficiency of the coating. In fact, Fig. 5 clearly shows that the u_e –pH or ζ –pH trends of composite particles of any composition are almost identical to those of the pure polymer. This points to the polymer shell very efficiently coating carbonyl iron, and leading to core/shell particles which, from the electrokinetic point of view, are indistinguishable from PBCA. In order to confirm these results, we also measured the mobility as a function of KNO_3 concentration at a constant pH = 5. The results of this analysis are plotted in Fig. 6, and one can observe how similar the electrokinetics of polymer and core/shell particles is, and how different from that of carbonyl iron. These results are in agreement with our previous studies on magnetite/poly(ethyl-2-cyanoacrylate) (core/shell) nanoparticles [10].

3.5. Surface thermodynamics

As mentioned, the surface free energy components (γ_S^{LW} , γ_S^+ , γ_S^-) of the three types of particles constitute a set of physical quantities which can also be analyzed to check the nature of PBCA coating. The contact angles of the three probe liquids on pellets obtained with the particles are detailed

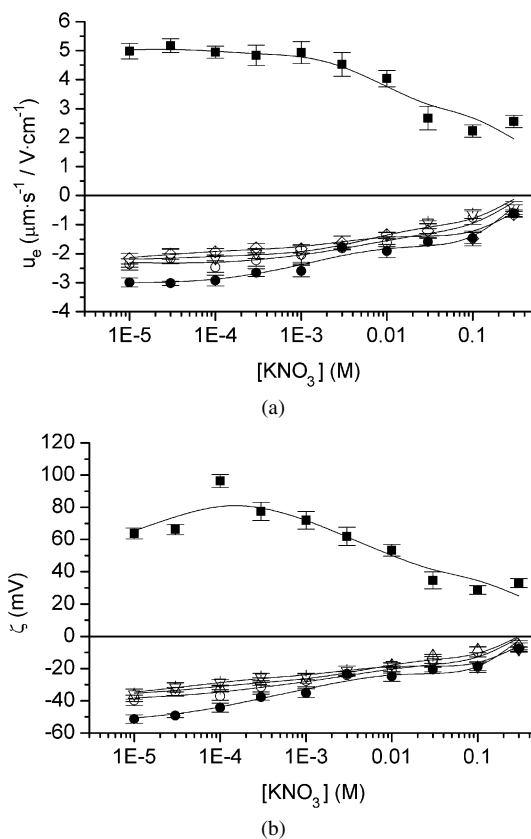


Fig. 6. Electrophoretic mobility (a) and zeta potential (b) of carbonyl iron (■), poly(butylcyanoacrylate) (●), and composite particles [of different initial monomer/carbonyl iron weight ratio: 4/3 (▽), 4/2 (△) and 4/1 (○)] as a function of the concentration of KNO_3 at pH 5.

Table 2

Contact angle θ (degrees) of the probe liquids indicated on carbonyl iron, poly(butylcyanoacrylate) (PBCA), and carbonyl iron/PBCA (core/shell) particles obtained for different proportions of monomer and carbonyl iron

Solid	Contact angle θ (degrees)		
	Water	Diiodomethane	Formamide
Carbonyl iron	27.1 ± 1.7	17.2 ± 0.7	21.5 ± 1.9
PBCA	73.1 ± 1.8	43.6 ± 2.4	56.9 ± 2.4
PBCA/Fe ⁰ (4/1)	83 ± 3	46 ± 3	58 ± 4
PBCA/Fe ⁰ (4/2)	84 ± 3	47.9 ± 2.9	57 ± 3
PBCA/Fe ⁰ (4/3)	80.3 ± 2.2	44.2 ± 1.8	58.0 ± 2.3

Table 3

Surface free energy components of carbonyl iron, PBCA and carbonyl iron/PBCA particles obtained for different proportions of monomer and carbonyl iron. γ_S^{LW} is the Lifshitz–van der Waals component; γ_S^+ (γ_S^-) is the electron-acceptor (electron-donor) component. All values in mJ/m^2

Solid	γ_S^{LW}	γ_S^+	γ_S^-
Carbonyl iron	48.5 ± 0.2	0.12 ± 0.02	46.8 ± 0.7
PBCA	37.7 ± 1.2	0.04 ± 0.02	11.7 ± 0.6
PBCA/Fe ⁰ (4/1)	36.6 ± 1.5	0.29 ± 0.14	4.0 ± 0.5
PBCA/Fe ⁰ (4/2)	35.4 ± 1.6	0.64 ± 0.09	2.7 ± 0.6
PBCA/Fe ⁰ (4/3)	37.4 ± 1.0	0.17 ± 0.04	5.5 ± 0.7

in Table 2. Even these raw contact angle data already suggest significant differences among the three types of nanoparticles. But it is the evaluation of the γ_S components, given in Table 3,

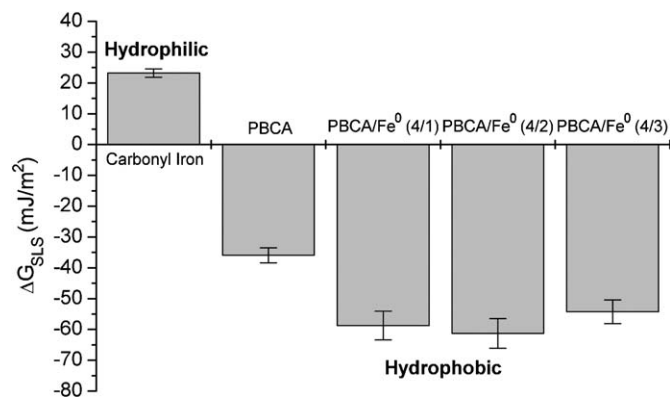


Fig. 7. ΔG_{SLS} values [Eq. (4)] and hydrophobicity/hydrophilicity of the three types of particles: carbonyl iron, poly(butylcyanoacrylate) and composite particles (of different initial monomer/carbonyl iron weight ratio: 4/3, 4/2 and 4/1).

that provides a better physical picture of the thermodynamics of the three kinds of surfaces. This table confirms to a great extent our estimations based on electrokinetic properties: the main conclusion that can be reached from these data refers to the fact that, whatever the component considered, its values for the composite particles are similar to those for the polymer (the electron-acceptor component, γ_S^+ , is not suitable for the comparison, as it displays small values in the three cases). In addition, the Lifshitz–van der Waals component of the mixed particles is almost the same as that of the cyanoacrylate polymer, although this component is the least affected (as is usually the case, see, e.g., Ref. [40]). The electron-donor component γ_S^- shows large values in carbonyl iron (like in many other inorganic oxides, for instance hematite, yttria and magnetite, as found in Refs. [10,40]), that is thus essentially a monopolar, electron-donor material. Its value of γ_S^- is much larger than that found for the polymer and for the composites. This thermodynamic analysis agrees with the electrokinetic one in suggesting that the coverage has been complete, since the components of γ_S for mixed particles coincide almost exactly with those corresponding to PBCA. This is true whatever the initial relative weights of monomer and carbonyl iron.

These surface free energy changes manifest themselves in the hydrophobicity/hydrophilicity characteristics of the different materials. According to van Oss et al. [27], a quantitative criterion may be used to check whether a material can be considered hydrophobic or hydrophilic, based on the evaluation of the free energy of interaction (not considering the electrostatic component), ΔG_{SLS} , between the solid phases immersed in the liquid. This can be written, per unit area of interacting particles, as follows:

$$\Delta G_{SLS} = -2\gamma_{SL}^{TOT}. \quad (4)$$

If this quantity is found to be negative, interfacial interactions will favor attraction of the particles to each other, and they are considered hydrophobic. In the opposite case, hydrophilicity will correspondingly be associated to positive values of ΔG_{SLS}^{TOT} . Fig. 7 shows the results for the three kinds of particles. As observed, the hydrophilic nature of carbonyl iron is modified and becomes hydrophobic (just like the polymer) when

they are covered by PBCA. This is found no matter what the monomer/nucleus ratio used in the synthesis is.

3.6. Mechanism of formation of the polymer layer

Considering all the information described about the surface characteristics of the materials involved, some arguments can be given concerning the mechanisms through which the polymer layer is formed on the carbonyl iron surface. First, it is clear that an attractive electrostatic interaction will exist between the positively charged carbonyl iron particles (see Fig. 5; recall that in the acid conditions in which the synthesis is performed, iron is positively charged) and the negatively charged carbanions. Because of this attraction, the vicinity of the carbonyl iron surface will be enriched in polymeric species. Surface thermodynamic arguments can additionally be given: from data in Table 3, the free energy of interaction between magnetic nuclei (M) and polymer (P) in the aqueous solution (S), ΔG_{MSP} , can be calculated using the Dupré equation [27]:

$$\Delta G_{MSP} = \gamma_{MP} - \gamma_{MS} - \gamma_{PS}, \quad (5)$$

where the interfacial free energies are given by Eq. (2) for each pair of interfaces involved. The result of the calculation is -4.8 ± 0.7 mJ/m². We can conclude that van der Waals and acid–base interactions between carbonyl iron and polymer are attractive, and this renders thermodynamically favored a process in which the polymer is in contact with the carbonyl iron.

4. Conclusions

In this work we have shown that it is possible to reproducibly coat magnetic colloidal spheres with a shell of the biodegradable polymer poly(butylcyanoacrylate), PBCA. Although the existence of the PBCA shell is observable under the electron microscope, the efficiency of the coating is demonstrated by the surface analysis of the mixed particles compared to that of their components. Such an analysis was performed by means of electrophoresis and contact angle measurements. Thus, the electrophoretic mobility of the composite particles changes with the pH and ionic strength in a very similar way as that of pure polymer. One can say that the electrical surface properties of carbonyl iron are almost completely controlled by the polymeric coating. Interestingly, surface thermodynamics analyses confirm this conclusion: the originally hydrophilic carbonyl iron changes to hydrophobic when coated by PBCA. These studies were carried out for different proportions of monomer and iron (from 4/3 to 4/1) in the starting synthesis reactions. Although for this range of compositions the differences between the properties of the composite particles are not very different, the optimum composition appears to be 4/3.

Acknowledgments

Butylcyanoacrylate from Henkel Loctite (Ireland) and financial support from CICYT, Spain, under Project MAT2005-07746-CO2-01, and from FEDER Funds are gratefully acknowledged.

References

- [1] P. Tartaj, M.P. Morales, S. Veintemillas-Verdaguer, T. González-Carreño, C.J. Serna, *J. Phys. D: Appl. Phys.* 36 (2003) R182.
- [2] Q.A. Pankhurst, J. Connolly, S.K. Jones, J. Dobson, *J. Phys. D: Appl. Phys.* 36 (2003) R167.
- [3] A.K. Gupta, M. Gupta, *Biomaterials* 26 (2005) 3995.
- [4] A.S. Lübbe, C. Alexiou, C. Bergemann, *J. Surg. Res.* 95 (2001) 200.
- [5] D.Q.M. Craig, in: R.B. McKay (Ed.), *Technological Applications of Dispersions*, Marcel Dekker, New York, 1994, chap. 13.
- [6] S. Goodwin, C. Peterson, C. Hoh, C. Bittner, *J. Magn. Magn. Mater.* 194 (1999) 132.
- [7] S.R. Rudge, T.L. Kurtz, C.R. Vessely, L.G. Catterall, D.L. Williamson, *Biomaterials* 21 (2000) 1411.
- [8] A.S. Lübbe, C. Bergemann, J. Brock, D.G. McClure, *J. Magn. Magn. Mater.* 194 (1999) 149.
- [9] A.S. Lübbe, C. Bergemann, H. Riess, F. Schiever, P. Reichardt, K. Possinger, M. Matthias, B. Dörken, F. Herrmann, R. Gürtler, P. Hohenberger, N. Haas, R. Sohr, B. Sander, A.-J. Lemke, D. Ohlendorf, W. Huhnt, D. Huhn, *Cancer Res.* 56 (1996) 4686.
- [10] J.L. Arias, V. Gallardo, S.A. Gómez-Lopera, R.C. Plaza, A.V. Delgado, *J. Controlled Release* 77 (2001) 309.
- [11] J.L. Arias, V. Gallardo, S.A. Gómez-Lopera, A.V. Delgado, *J. Biomed. Nanotech.* 1 (2) (2005) 1.
- [12] P. Whittaker, S.F. Ali, S.F. Imam, V.C. Dunkel, *Regul. Toxicol. Pharm.* 36 (2002) 280.
- [13] H.A. Huebers, G.M. Brittenham, E. Csiba, C.A. Finch, *J. Lab. Clin. Med.* 108 (1986) 473.
- [14] S.D. Devathali, V.R. Gordeuk, G.M. Brittenham, J.R. Bravo, M.A. Hughes, L.J. Keating, *Eur. J. Haematol.* 46 (1991) 272.
- [15] W. Chua-Anusorn, D.J. Macey, J. Webb, P. de la Motte Hall, T.G. St. Pierre, *Biometals* 12 (1999) 103.
- [16] E. Okon, D. Pouliquen, P. Okon, Z.V. Kovaleva, T.P. Stepanova, S.G. Lavit, B.N. Kudryavtsev, P. Jallet, *Lab. Invest.* 71 (6) (1994) 895.
- [17] E. Fattal, M.T. Peracchia, P. Couvreur, in: A.J. Domb, J. Kost, D.M. Wiseman (Eds.), *Handbook of Biodegradable Polymers*, Harwood Academic Publishers, Amsterdam, 1997, chap. 10.
- [18] G. Cavallaro, M. Fresta, G. Giammona, G. Puglisi, A. Villari, *Int. J. Pharm.* 111 (1994) 31.
- [19] N. Henry-Toulmé, A. Decout, J. Lalanne, F. Nemati, C. Dubernet, J. Dufourcq, *J. Colloid Interface Sci.* 162 (1994) 236.
- [20] Y.-P. Hu, S. Jarillon, C. Dubernet, P. Couvreur, J. Robert, *Cancer Chemother. Pharmacol.* 37 (1996) 556.
- [21] A. Decout, C. Dubernet, N. Henry-Toulme, *J. Colloid Interface Sci.* 181 (1996) 99.
- [22] F. Nèmati, C. Dubernet, H. Fessi, A.C. de Verdière, M.F. Poupon, F. Puisieux, P. Couvreur, *Int. J. Pharm.* 138 (1996) 237.
- [23] A. Ibrahim, P. Couvreur, M. Roland, P. Speiser, *J. Pharm. Pharmacol.* 35 (1983) 59.
- [24] M.E. Page, H. Pinto-Alphandary, E. Chachaty, A. Andremont, P. Couvreur, *STP Pharma Sci.* 6 (4) (1996) 298.
- [25] L. Montanaro, C.R. Arciola, E. Cenni, G. Ciapetti, F. Savioli, F. Filippini, L.A. Barsanti, *Biomaterials* 22 (2001) 59.
- [26] C. Lherm, R.H. Müller, F. Puisieux, P. Couvreur, *Int. J. Pharm.* 84 (1992) 13.
- [27] C.J. van Oss, *Interfacial Forces in Aqueous Media*, Marcel Dekker, New York, 1994.
- [28] C.J. van Oss, M.K. Chaudhury, R.J. Good, *Chem. Rev.* 88 (1988) 927.
- [29] J.D.G. Durán, A. Ontiveros, A.V. Delgado, F. González-Caballero, E.J. Chibowski, *Adhes. Sci. Technol.* 10 (1996) 847.
- [30] A.W. Adamson, *Physical Chemistry of Surfaces*, fifth ed., Wiley, New York, 1990.
- [31] H. Maeda, J. Fang, T. Inutsuka, Y. Kitamoto, *Int. Immunopharmacol.* 3 (2003) 319.
- [32] S. Goodwin, C. Peterson, C. Hoh, *J. Magn. Magn. Mater.* 194 (1999) 132.
- [33] R.M. Silverstein, F.X. Webster, *Spectrometric Identification of Organic Compounds*, sixth ed., Wiley, New York, 1998, chap. 3.
- [34] M.T. Peracchia, C. Vauthier, M. Popa, F. Puisieux, P. Couvreur, *STP Pharma Sci.* 7 (6) (1997) 513.
- [35] P.P. Phulé, M.T. Mihalcin, S. Gene, *J. Mater. Res.* 14 (1999) 3037.
- [36] R.W. O'Brien, L.R. White, *J. Chem. Soc., Faraday Trans. 2* (274) (1978) 1607.
- [37] N. Kallay, Ž. Torbić, M. Golić, E. Matijević, *J. Phys. Chem.* 95 (1991) 7028.
- [38] E. Matijević, in: A.V. Delgado (Ed.), *Interfacial Electrokinetics and Electrophoresis*, Marcel Dekker, New York, 2002, chap. 8.
- [39] R.H. Müller, C. Lherm, J. Herbort, T. Blunk, P. Couvreur, *Int. J. Pharm.* 84 (1992) 1.
- [40] R.C. Plaza, L. Zurita, J.D.G. Durán, F. González-Caballero, A.V. Delgado, *Langmuir* 14 (1998) 6850.